JOURNAL OF AIRCRAFT
Vol. 46, No. 1, January–February 2009

Effects of Vortex Generators on an Airfoil at Low Reynolds Numbers

Amith Seshagiri,* Evan Cooper,* and Lance W. Traub†
Embry-Riddle Aeronautical University, Prescott, Arizona 86301

DOI: 10.2514/1.36241

A low-speed wind-tunnel investigation is presented detailing the effects of vortex generators on an airfoil at low Reynolds numbers (80,000 and 160,000). Six different static vortex generator layouts were tested. In addition, an oscillatory (or active) vortex generator was designed and tested. Force balance measurements were recorded and interpreted with the aid of surface flow visualization. The data suggest that the static vortex generators function similarly to those at higher Reynolds numbers; increasing the maximum lift coefficient and increasing the stall angle. Different static vortex generator configurations appear preferable at the two tested Reynolds number ranges. The oscillating vortex generator did not appear effective in its present configuration.

Introduction

SMALL unmanned flight vehicles are seeing ever-increasing use in both military and civilian application. These flight vehicles can be used for real-time reconnaissance in high-threat areas or where a compact aircraft would be most effective. They can be used for border surveillance, wildlife management, search and rescue, and many other functions. Generally, these flight vehicles operate at low Reynolds numbers, often less than 200,000. A natural consequence of this low Reynolds number regime is comparatively poor airfoil performance, manifest in an increased minimum drag coefficient and reduced maximum lift coefficient.

Low Reynolds number airfoil flows are often dominated by the presence and behavior of laminar separation bubbles. Generally, for Reynolds numbers below 70,000, the flow is laminar, and methods to initiate transition may not be effective. The length of the laminar separation bubble is typically longer than the length of the airfoil aft of the separation line, and so reattachment does not occur [1]. However, in low Reynolds number flows, a general description of behavior is complicated by individual airfoils potentially exhibiting performance outside the generalization; a study by Selig et al. [2] showed that a zigzag pattern trip strip was effective in promoting transition on a SD8020 section, eliminating the nonlinear behavior of the clean section for $Re = 40,000$ and 80,000. The poor separation resistance of the laminar boundary-layer complicates low Reynolds number airfoil design. As the Reynolds number is increased to 100,000, methods to initiate transition may become more effective. The separated laminar shear layer may naturally transition to turbulence, promoting turbulent reattachment (through entrainment and enhanced mixing). Increasing the section's angle of attack usually causes the bubble to move forward (due to the increasing pressure recovery demands aft of the minimum pressure location) with little change in its length [2]. As the Reynolds number is increased, a short bubble may form that has a lesser effect on the local pressure distribution. Generally, an increase in Reynolds number results in a shortening of the bubble; the laminar separation point stays approximately constant but the reattachment point moves upstream [3,4]. However, increasing angle of attack may see this short bubble burst, forming either a long bubble or failing to reattach at all [1]. This results in a sharp or abrupt stall with significant lift, moment, and drag implications.

A common method to promote boundary-layer transition is a trip strip consisting of either distributed roughness (grit) or some type of patterned tape (e.g., aluminum tape with a cut zigzag pattern). Trip strips are commonly used in low Reynolds number testing as a means of lessening scale effects. For very low Reynolds number testing, trip strips may not be totally effective. A study of the Voyager canard by Bragg and Gregorek [5] to explore effects of contamination showed that a boundary-layer trip degraded performance significantly. Trip strips are used to promote laminar-turbulent transition such that the turbulent boundary layer can overcome the adverse gradients that would otherwise cause laminar separation.

Vortex generators (VGs) have been widely employed to energize "sluggish" boundary layers, which are usually turbulent and thick. Their purpose is to delay the onset of flow separation and consequently increase the maximum lift coefficient. The VG themselves are typically small inclined vanes that may be rectangular or triangular in shape. They work by generating streamwise vortices that are effective at mixing high-energy freestream fluid into the lower extents of the boundary layer, thus energizing it. VGs are usually designed to be approximately half the height of the local boundary-layer thickness [6]. Simple and inexpensive to implement, VGs do have drawbacks: they increase the minimum drag and may decrease the maximum lift-to-drag ratio. However, the maximum lift coefficient is usually increased and the angle of attack of stall is delayed. In the aforementioned study by Bragg and Gregorek [5], VGs were also evaluated and were found to improve the degraded performance due to the trip strip back to the "clean section" level (the study was to investigate contamination, simulated through the grit-type trip strip). Wheeler-type vortex generators have shown a lesser drag penalty than typical vortex generators for similar levels of flow control [7]. Their design is, however, slightly more complicated than typical vane-type VGs.

Active flow control has matured over the last two decades, as is evidenced by the numerous studies validating its effectiveness over passive means [8–10]. Active flow control is exemplified by the synthetic jet actuator [9,10], a zero-mass-flux finite momentum flow effecter. Synthetic jets create an oscillatory jet that is usually injected tangentially into the boundary layer. If pulsed at the correct frequency, the forcing can cause the separating shear layer to become resonant, causing it to roll up and form discrete vortical structures that advect over the upper wing surface. Similar to VGs, they draw high-energy freestream fluid down to the wing's surface. The advantage of oscillation is a significant reduction in the required jet momentum to achieve a desired delay in stall angle or maximum lift compared with steady blowing. Studies have also demonstrated that a vortex generator that is cyclically deployed may also have unsteady

Received 17 December 2007; revision received 15 February 2008; accepted for publication 16 February 2008.

*Undergraduate Student, Aerospace and Mechanical Engineering Department.

†Associate Professor, Aerospace and Mechanical Engineering Department. Member AIAA.

benefits. Tests [11] have demonstrated the ability to achieve flow control superior to their stationary counterparts.

Little information is available on the effect of VGs at low Reynolds numbers (less than 200,000). A study by Nickerson [12] on the effects of VGs at low Reynolds numbers showed a delay in the onset of stall, but a reduction in the maximum lift coefficient. The ability of VGs to increase maximum lift would be of great value in the challenging low Reynolds numbers environment. In this paper, an experimental wind-tunnel investigation is reported showing the effect of VGs on an airfoil at low Reynolds numbers. This is an environment in which the extreme simplicity and low weight of these devices may make them more attractive than existing active flow control solutions. Static vane-type generators are evaluated in various configurations. Additionally, an active VG is designed and tested. The study aims to establish if static VGs are effective at Reynolds numbers below 200,000 and if an oscillating VG yields benefits. Data presentation includes force balance as well as surface flow visualization.

Equipment and Procedure

A low-speed, 1 by 1 ft, open-return wind tunnel was used. The tunnel has a maximum velocity of 45 m/s. Velocity uniformity within the jet is within 0.2%. The wing (see Fig. 1a) was designed in CATIA and then rapid-prototyped using Embry-Riddle's rapid-prototyping facilities, yielding an ABS (acrylonitrile butadiene styrene) plastic wing representation. The wing had a chord of 165 mm. The section was a NASA Langley Research Center LS(1)-0417 GA(W)-1 with a thickness of 17%. The profile was chosen due to its good performance at low Reynolds numbers and its large volume to accommodate the oscillatory drive mechanism. The wing had a span of 101.6 mm. To simulate quasi-2-D flow, a full height splitter plate was mounted next to the wing. The wing had an upper-section insert that contained the VGs. Six different stationary VG configurations were evaluated (see Fig. 1b). VG1 corresponds to the clean wing. Each configuration had an insert plate that was inserted into the wing for testing. All the stationary VG were essentially thin (approximately 0.2 mm) rectangular vanes that projected 2 mm above the wing surface. Four of the VG configurations would generate corotating vortices (VG2, VG4, VG6, and VG7) and two contrarotating vortices (VG3 and VG5) (see Fig. 1b).

As oscillatory blowing has proven to be highly effective, by analogy, active VGs may also show benefit and were consequently designed. The oscillation mechanism is shown in Fig. 1a. An electric motor turns an elliptical cam. The cam in turn depresses a lever attached to the VG supporting rod. The lever rebounds and stays in contact with the cam due to the placement of an elastic stop. The VGs used were triangular in shape, as may be seen in the figure. They were located 20% from the leading edge. This location was dictated by geometric and manufacturing considerations. The leading-edge sweep angle was 60 deg with a chord of 5 mm. This configuration was used because it was the simplest to implement and allowed the VGs to conformally close against the wing surface when not actuated, thus minimizing any drag penalty. Oscillation frequency was measured using an Optek IR pickup connected to a Fluke multimeter with a frequency function. Testing showed the system could oscillate at over 250 Hz. When fully deployed, the VGs projected up 1 mm, yielding an incidence angle of 18 deg relative to the surface.

Forces and moment were measured using an ATI Mini-43 six-component force balance. The balance was selected due to its small load range (36 N full scale), to maximize measurement accuracy. The balance was mounted in a rotatable wall plug and was attached to a rod that cantilevered the model into the test section. Consequently, the balance measured loads in a body-axis reference frame. Repeated data runs suggested accuracy within ± 0.01 and ± 0.006 for the lift and drag coefficients, respectively. These values correspond to accuracy within 0.83 and 1.9% for the lift and drag coefficients, respectively, in the vicinity of the maximum lift coefficient.

Surface flow visualization was performed using a mixture of titanium dioxide, paraffin, linseed oil and oleic acid. The wing was set at the desired angle of attack (AOA), the mixture was applied using a brush, and the tunnel was rapidly increased to the desired Reynolds number. The fluid motion was observed to aid in interpretation while still and video images were recorded. Random test conditions were repeated to determine pattern repeatability. Surface visualization was undertaken for AOA $= 0$ and 14 deg.

The tunnel freestream velocity was measured using a FlowKinetics LLC FKT 1DP1A-SV meter. This meter measures atmospheric pressure, temperature, and relative humidity, all of which are used to compute the density used in the velocity calculation. Meter accuracy is specified by the manufacturer as better than 0.1%. The wing angle of attack was set using a Mitutoyo 3600 digital protractor with a resolution of 0.01 deg. Wing set repeatability was also found to be within 0.1 deg. As the tests are essentially comparative, no corrections for wall effects were applied.

Results and Discussion

Force balance data are presented in Figs. 2–7, a flow visualization summary is presented in Fig. 8, and additional balance data are presented in Figs. 9–13. Figure 2 presents a repeated data run with the clean wing at $Re = 160,000$. The effect of the static vortex generators for $Re = 80,000$ is shown in Fig. 3. Like configurations are grouped by symbol type, and symbol solidity indicates VG angle (hollow symbols have vane angles of 15 deg and solid are 25 deg). The data show that the VGs improve lifting performance, reflected in an increase in lift-curve slope and the maximum lift coefficient. The surface flow visualization data (Fig. 8) indicates that the VGs reduce the extent of the laminar separation bubble and, for some VG configurations, effectively section the bubble into segments. A fairly large bubble over the upper aft section of the airfoil can have the effect of decambering the profile by increasing the displacement thickness significantly, reducing the lift for a given angle of attack. The minimization of the bubble may thus lessen this effect. Staggering the VGs (VG4 and VG6) shows the poorest performance of the tested configurations. The data also show that the lowest blade angle, 15 deg, yields better performance than 25 deg. This suggests that at this Reynolds number, a blade angle of 25 deg effectively generates a weaker vortex than that at 15 deg. This is also supported by the surface flow visualization (i.e., compare VG3 and VG5 at a 0 deg AOA for $Re = 80,000$). The surface scrubbing appears more defined for the lower incidence blades, as does the persistence and penetration of the vortices through the separation bubble.

The effect of the VGs at $Re = 160,000$ is shown in Fig. 4. The data are qualitatively similar to the well-established effect of VGs (i.e., an increase in the maximum lift coefficient and stall angle). Of note is a significant lift coefficient increase with respect to the clean wing from approximately 0.2 below the maximum lift coefficient onward. In this Reynolds number regime, all generator configurations appear to provide performance enhancement. Performance differences between the particular VG configurations are marginal; however, it appears that the 25 deg blade incidence offers better performance than the 15 deg (as opposed to the $Re = 80,000$ case). Surface flow evidence at $Re = 160,000$ is suggested by comparison of VG4 and VG6; the greater blade angle (VG4) shows more defined vortices, which indicates greater vortex strength for similar test conditions.

Effects of the VGs on the measured drag coefficient at $Re = 160,000$ are presented in Fig. 5. Drag coefficient plots for $Re = 80,000$ are omitted due to uncertainty of the accuracy or reliability of the data. The data shows that all VG configurations appear to have reduced zero lift drag compared with the clean wing. This result is most likely due to the VGs partially eliminating the large upper surface laminar separation bubble (see Fig. 8). Thus, the drag reduction is one of pressure, not skin friction. The polar shows that drag increases more rapidly for most VG configurations than the clean section. This trend is explored by plotting the linearized drag polar (Fig. 6, in which the drag coefficient is plotted as a function of the square of the lift coefficient). For an airfoil, the slope of the polar then relates to the buildup of pressure drag; a lower slope indicates reduced pressure drag generation for the profile. Figure 6 clearly

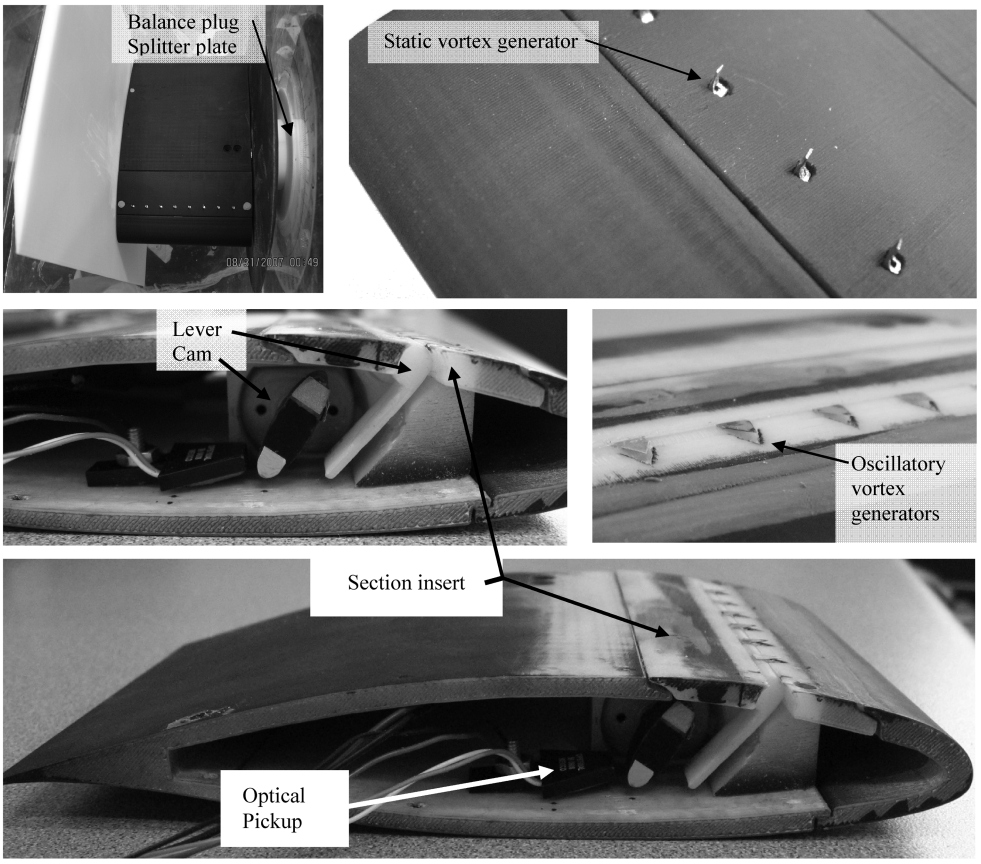

a)

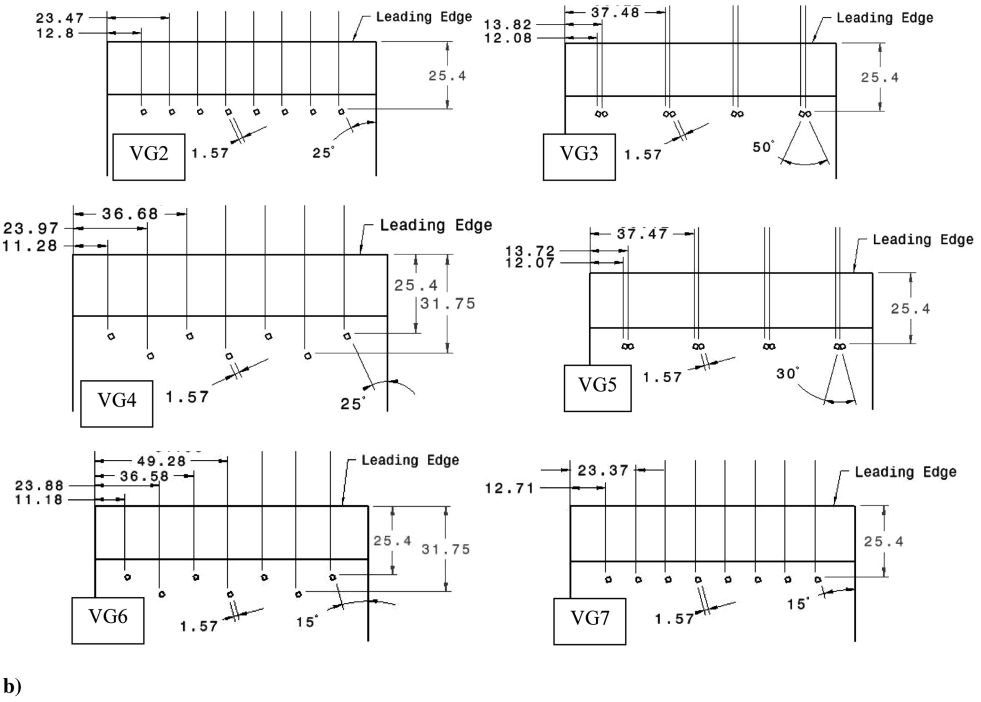

b)

Fig. 1 Wind-tunnel model details: a) model and VG installation and b) vortex generator designation and layout (VG1 is the clean wing).

shows that all VG configurations have slope that is greater than or equal to that of the clean profile (i.e., kp_1). This suggests that the VGs may lessen drag at low AOA by limiting the extent of the bubble (so reducing pressure drag). As incidence increases and the bubble naturally shifts forward, the pressure drag penalty for the clean wing diminishes, but the increased drag caused by the VGs is still present, causing a greater perceived pressure drag buildup.

A summary of the maximum lift coefficient increment (or decrement) for each VG configuration compared with the clean wing is shown in Fig. 7. The data suggest that for the tested VG configurations, the higher Reynolds numbers tests show greater performance enhancement. VG5, which generates closely paired counter-rotating vortices, appears to show the best overall performance of the tested configurations.

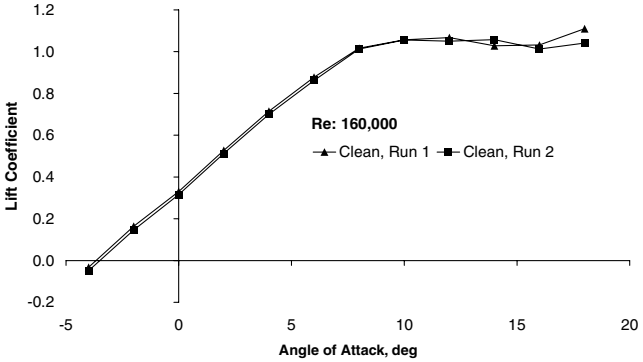

Fig. 2 Repeated data run for the clean wing at $Re = 160,000$.

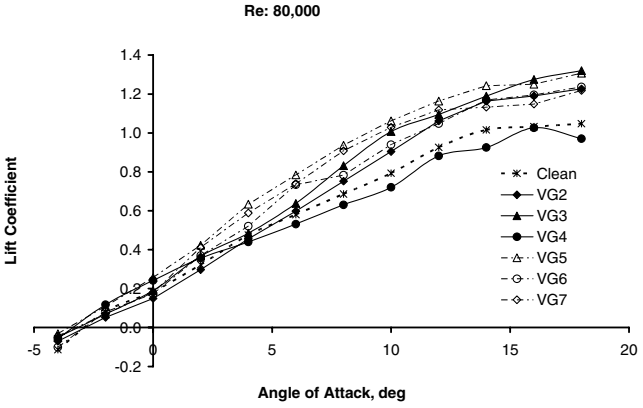

Fig. 3 Effect of static vortex generators on measured lift coefficient at $Re = 80,000$.

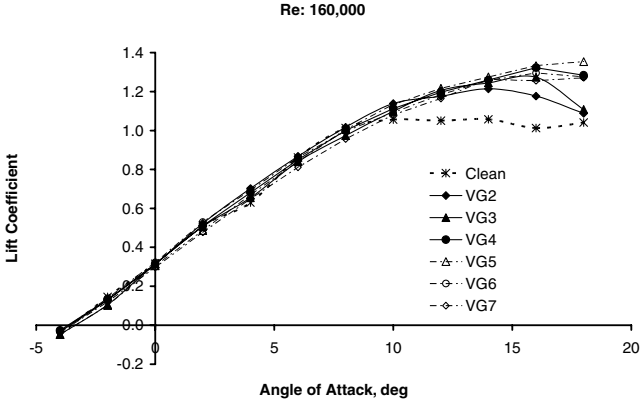

Fig. 4 Effect of static vortex generators on measured lift coefficient at $Re = 160,000$.

Surface flow visualization summaries are presented in Fig. 8. The patterns were recorded at 0 and 14 deg AOA for $Re = 80,000$ and 160,000. Because of space considerations and the similar appearance of many VG configuration surface flows, only selected examples are presented. The clean wing (VG1) indicates the presence of a large laminar bubble extending from approximately 55% aft. Increasing the Reynolds number from 80,000 to 160,000 has the effect of shortening the bubble without significantly altering the laminar separation location as noted in other studies [3]. As most VG configurations appear to have similar effects, their behavior will be discussed in collective manner. At a 0 deg AOA, the vortex generators are seen to essentially have the effect of splicing the separation bubble into streamwise segments; thus, its extent is reduced, but the bubble is not eliminated. Increasing the angle of attack to 14 deg shows a forward movement and contraction of the

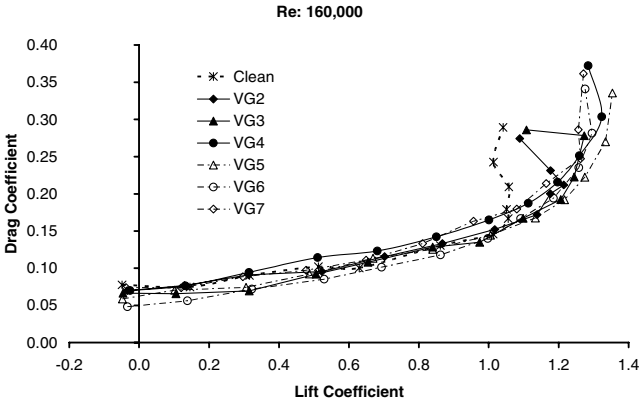

Fig. 5 Effect of static vortex generators on measured drag coefficient at $Re = 160,000$.

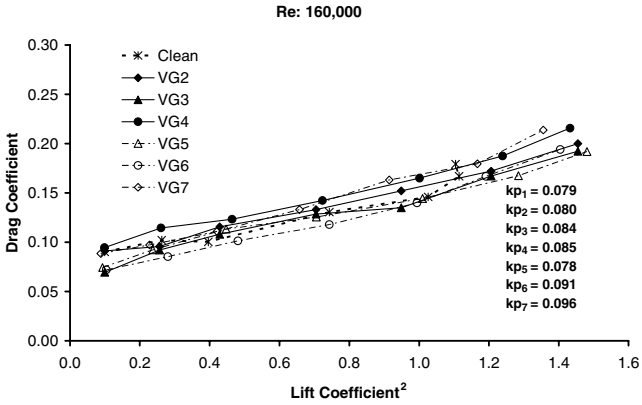

Fig. 6 Effect of static vortex generators on linearized drag polar at $Re = 160,000$.

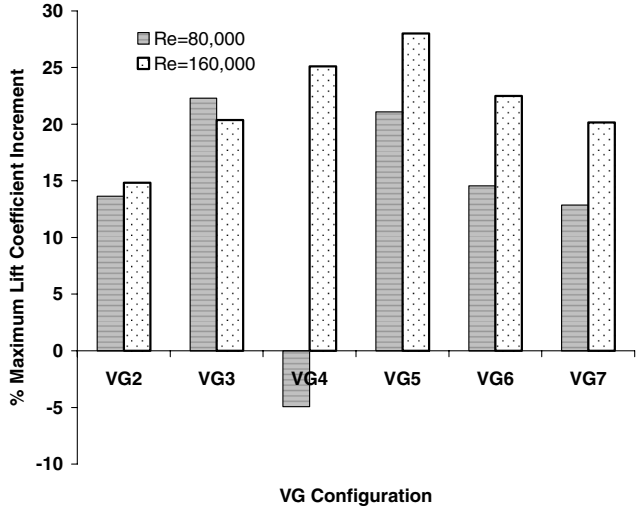

Fig. 7 Lift coefficient increment summary for $Re = 80,000$ and 160,000.

bubble. The bubble extends from approximately 5 to 17% of the chord. As may be seen for $Re = 80,000$, the bubble reattachment location may be aft of the VG locations. Consequently, when operating at low Reynolds numbers, it is unlikely that a single fixed chordwise VG location will suffice. At a 14 deg angle of attack, comparison of the surface flow with VGs to the clean wing indicates reduced areas of separation, reflected in the greater lift shown in Fig. 4. All figures clearly show a transition bubble followed by a turbulent trailing-edge separation stall mechanism.

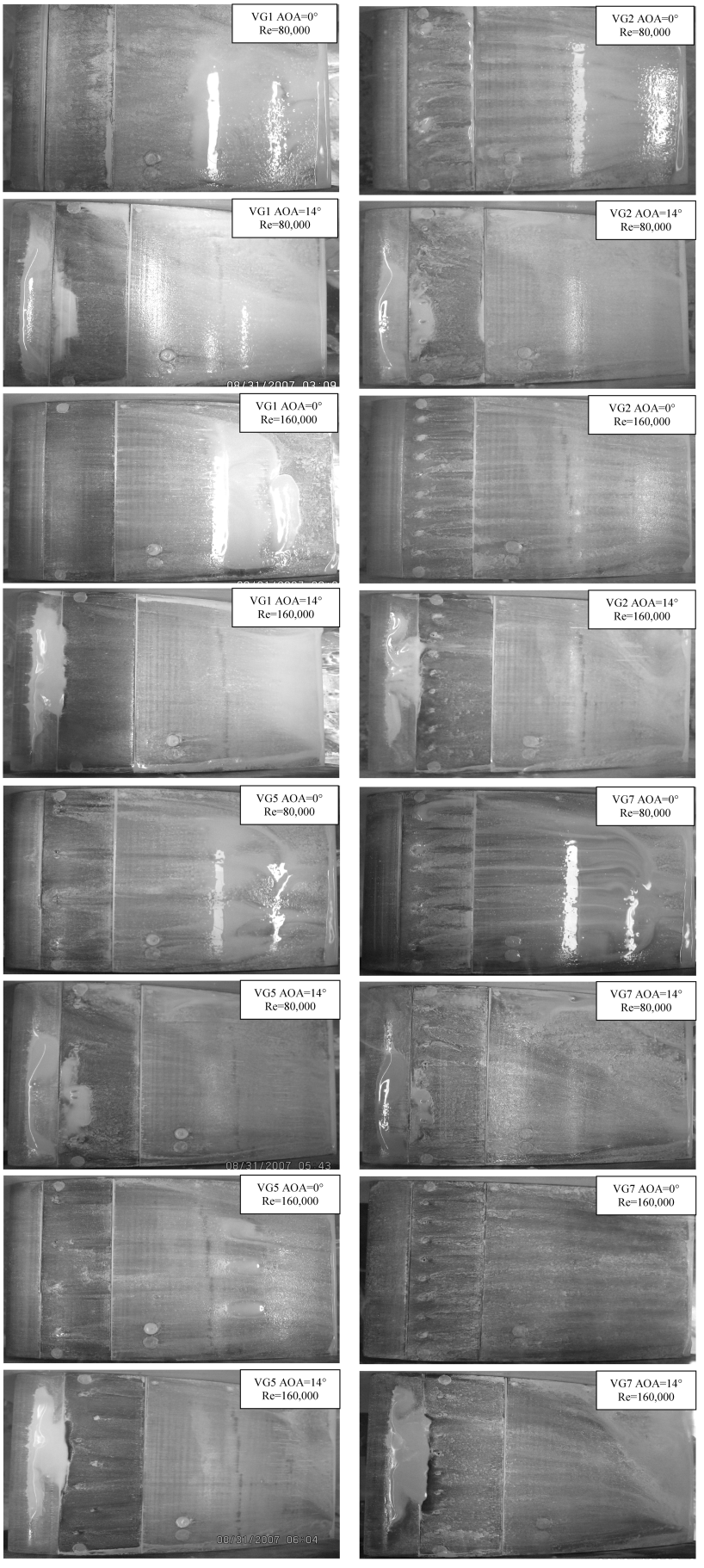

Fig. 8 Surface flow skin friction pattern summary.

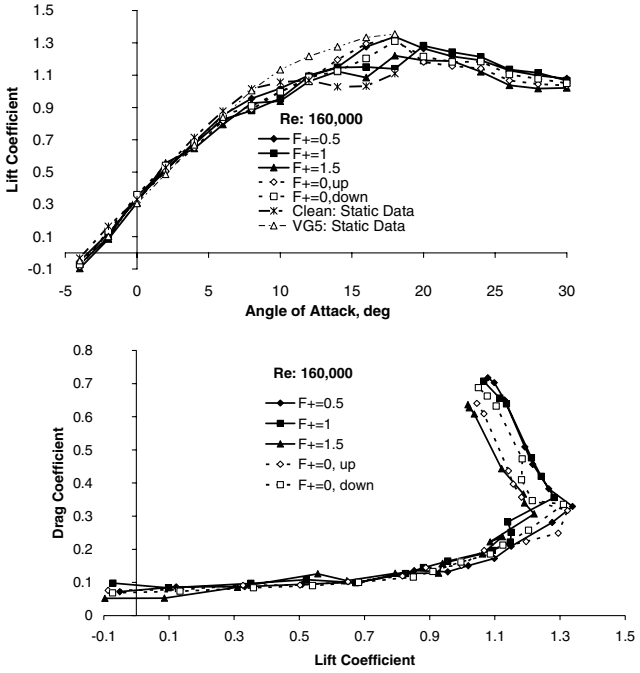

Fig. 9 Effect of active VGs on measured lift and drag coefficient at $Re = 160,000$.

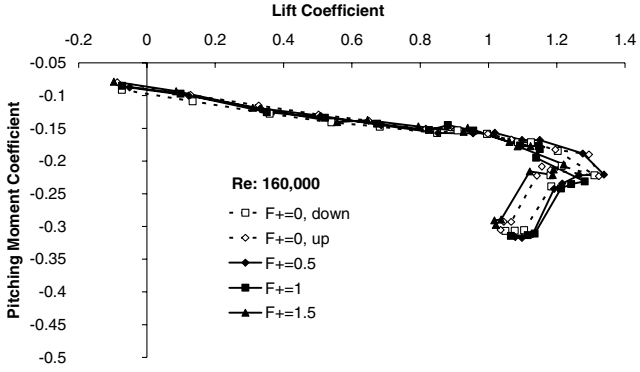

Fig. 10 Effect of active VGs on measured pitching moment coefficient at $Re = 160,000$.

Active flow control studies [8–10] have indicated that a Strouhal number or nondimensional oscillation frequency of approximately 1 yields the best performance. For synthetic jet actuators, this corresponds to 2–4 advecting upper surface vortical structures. Consequently, in the present study, the delta-shaped VGs were oscillated at $F+ = 0.5$, 1, and 1.5, corresponding to actual frequencies of 68, 136, and 204 Hz at the test freestream velocity ($F+ = fx/U$, where f is the oscillation frequency, x is the distance from the actuator to the trailing edge, U is the freestream velocity, and $F+$ is the nondimensional oscillation frequency). Figures 9 and 10 show the effects on lift, drag, and pitching moment coefficient. In these presented data, the $F+ = 0$ down (i.e., the VG was flush with the surface) may be construed as the clean case. The data suggest that, as implemented, the active VGs are ineffective compared with the $F+ = 0$ down case. However, a comparison of the data with the earlier static test case result shows that all of the tests with the active VG configuration, whether actuated up or down, show enhanced lift at high AOA compared with the earlier static case (clean static data). It is thus possible that the active VG implementation, whether deployed or not, was enhancing mixing and reducing the extent of trailing-edge separation. The surface patterns in Fig. 8 indicate that for AOA ≥ 14 deg, the VGs are most likely immersed in a turbulent boundary layer following bubble reattachment. The most effective

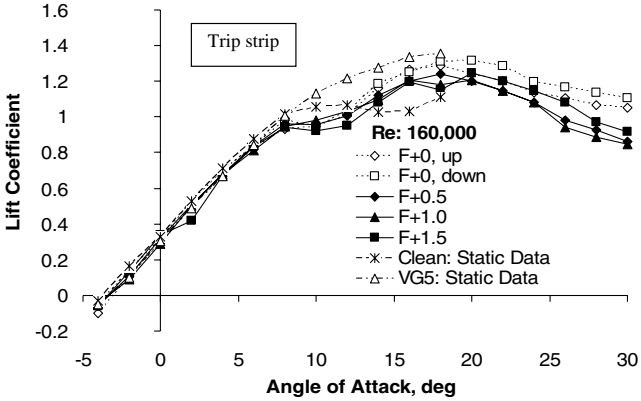

Fig. 11 Effect of active VGs on measured lift coefficient at $Re = 160,000$; trip strip is located at 6% chord.

static VG, VG5, is also included in the data presentation. It is apparent that this passive VG shows the best performance recorded for all test configurations. Of the active cases, the data suggest that increasing $F+$ degrades performance. It should be mentioned that the static VGs projected up twice the height of the oscillatory VG. It is also apparent in Fig. 9 that at around an 8 to 10 deg angle of attack, all of the $F+$ data sets show a lift "dip," compared with the earlier static data.

The drag polar (lower inset in Fig. 9) and the pitching moment plot (Fig. 10) do not indicate any clearly identifiable effects of the active VGs. The apparently poor performance of the active VGs may be attributable to their design. The leading-edge sweep angle of the VGs was 60 deg. This would generate a vortex that would burst at a comparatively low vortex generator inclination [13]. In these tests, the maximum VG angle was approximately 18 deg, an incidence that would result in vortex breakdown. Consequently, the well-defined leading-edge vortical structures with concentrated cores of high vorticity would break down to turbulence and not penetrate effectively downstream. The active VGs should have been larger and of higher sweep (although this reduces the vortex circulation for a given incidence, it delays the onset of vortex bursting).

To potentially explore means to improve the behavior of the existing active VG implementation, a trip strip was positioned at 6% of the wing chord from the leading edge. The concept was that if the bubble can be eliminated, the boundary layer that the active VGs are immersed in at high angles of attack would be reduced in thickness (compared with the turbulent boundary layer following bubble reattachment), such that the VGs may penetrate into the higher-energy freestream. Results and computations are shown in Figs. 11–13. The lift plot with trip strip now shows a clear apparent plateau from approximately 8 to 10 deg, similar to that seen in Fig. 9, but more defined. To clarify this effect, simulations were run using XFOIL [14] with natural transition. Results are shown in Fig. 12. Although the magnitudes do not match, the computational data shows the same characteristic. Pressure traces included in Fig. 12 show that the plateau is associated with a fairly rapid forward movement of the laminar separation bubble. This suggests that the trip strip was not effective in promoting transition; it may also be seen that its 6% location is imbedded in the strong favorable pressure gradient at the nose. The disparity between that data in Figs. 9 and 11 and the static VG data in Fig. 4 may be due to the surface finish of the section insert plate. It was smoothly faired-in using clay for the oscillatory VG cases, whereas this was not so for the static test cases. Thus, the two junctions of this plate and the wing may have caused, or at least promoted, transition at higher wing AOA (due to the corresponding greater adverse pressure gradients). This would affect the existence of the bubble until the location of laminar separation moved in front of the section insert plate. Recorded drag coefficient data have not been included due to a potential lack of reliability of the results. Although slight, vibration of the active VG actuator affected the repeatability of the drag data, but had no perceivable effect on the lift or pitching moment coefficient. Actuation does not appear to have

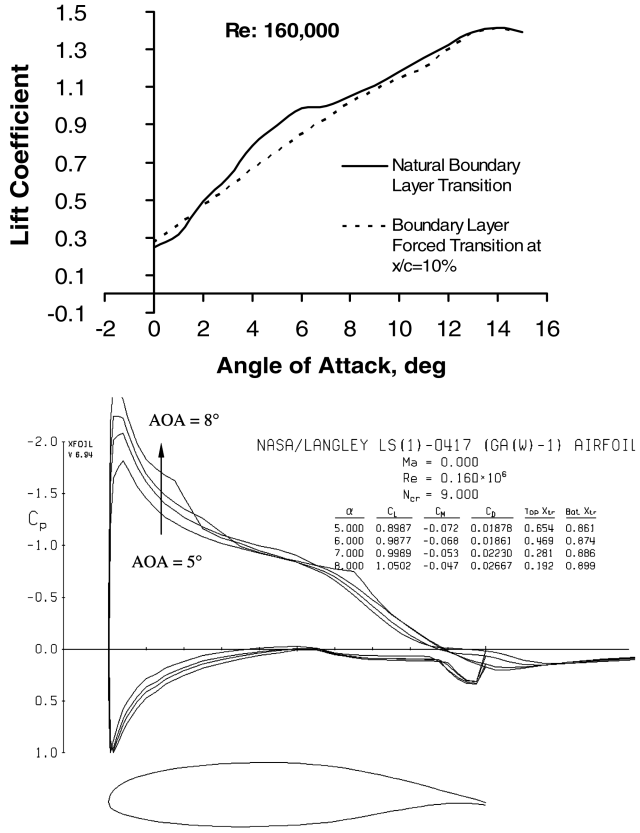

Fig. 12 Xfoil lift and pressure estimates; pressure distributions assume a natural transition.

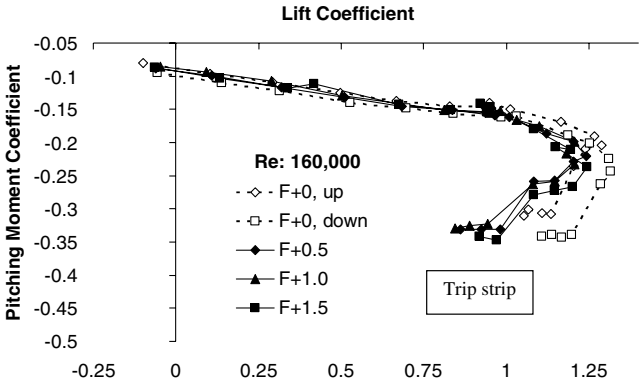

Fig. 13 Effect of active VGs on measured pitching moment coefficient at $Re = 160,000$.

a significant effect on pitching moment coefficient, as may be seen in Fig. 13.

Conclusions

A low-speed wind-tunnel investigation was undertaken to determine the effect of vortex generators at low Reynolds numbers (80,000 and 160,000). Six different static configurations were evaluated; some generating corotating and others generating contrarotating vortices. In addition, an active oscillatory vortex generator was designed and manufactured. Force balance and surface flow visualization data were recorded. The results indicated that the static vortex generators were able to increase the maximum lift coefficient up to 25%, whereas greater augmentation was seen at $Re = 160,000$ than at $Re = 80,000$. Visualization indicated that the vortex generators did not eliminate the laminar separation bubble, but reduced its extent by splicing it into segments. Within the present data, the most effective vortex generator blade settings were generally different for $Re = 80,000$ and 160,000; however, the paired counter-rotating vortex generators arranged at a 30 deg blade angle were the most effective tested arrangement. In the present implementation, the active vortex generators did not show any performance improvement over their static counterparts.

Acknowledgements

The authors would like to acknowledge support from Embry-Riddle University, who provided support for Amith Seshagiri and Evan Cooper through an internal grant during the conduct of this research. The authors would like to thank Joshua Johnston for his initial work on this project. Additionally, the authors would like to thank the Associate Editor and reviewer for their comments and suggestions.

References

[1] Lissaman, P. B. S., "Low-Reynolds-Number Airfoils," *Annual Review of Fluid Mechanics*, Vol. 15, 1983, pp. 223–239. doi:10.1146/annurev.fl.15.010183.001255

[2] Selig, M. S., Guglielmo, J. J., Broeren, A. P., and Giguere, P., "Experiments on Airfoils at Low Reynolds Numbers," AIAA 34th Aerospace Sciences Meeting, Reno, NV, AIAA Paper 96-0062, Jan. 1996.

[3] Traub, L. W., and Cooper, E., "An Experimental Investigation of Pressure Measurement and Airfoil Characteristics at Low Reynolds Numbers," *Journal of Aircraft*, Vol. 45, No. 4, 2008, pp. 1322–1333. doi:10.2514/1.34769

[4] Hsiao, F. B., and Hsu, C. C., "Numerical Prediction of Aerodynamic Performance for Low Reynolds Number Airfoils," *Journal of Aircraft*, Vol. 26, No. 7, 1989, pp. 689–691. doi:10.2514/3.45823

[5] Bragg, M., and Gregorek, G. M., "Experimental Study of Airfoil Performance with Vortex Generators," *Journal of Aircraft*, Vol. 24, No. 5, 1987, pp. 305–309. doi:10.2514/3.45445

[6] Kerho, M. F., "Enhanced Airfoil Design Incorporating Boundary Layer Mixing Devices," 41st AIAA Aerospace Sciences Meeting and Exhibit, Reno, NV, AIAA Paper 2003-0211, Jan. 2003.

[7] Barrett, R., and Farokh, S., "On the Aerodynamics and Performance of Active Vortex Generators," AIAA Paper 93-3447-CP, 1993.

[8] Traub, L. W., Miller, A. C., and Rediniotis, O. K., "Effects of Active and Passive Flow Control on Dynamic Stall Vortex Formation," *Journal of Aircraft*, Vol. 41, No. 2, 2004, pp. 405–408. doi:10.2514/1.2591

[9] Traub, L. W., Miller, A. C., and Rediniotis, O. K., "Effects of Synthetic Jet Actuation on a Ramping NACA 0015 Wing," *Journal of Aircraft*, Vol. 41, No. 5, 2004, pp. 1153–1162. doi:10.2514/1.3500

[10] Gilarranz, J. L., Traub, L. W., and Rediniotis, O. K., "Characterization of a Compact, High-Power Synthetic Jet Actuator for Flow Separation Control," AIAA Paper 2002-0127, Jan. 2002.

[11] "Active Flow Control," *Applications* [online database]http://www.flxsys.com/Applications/ [retrieved 26 Nov. 2007].

[12] Nickerson, J. D., "A Study of Vortex Generators at Low Reynolds Numbers," 24th AIAA Aerospace Sciences Meeting, Reno, NV, AIAA Paper 1986-155, Jan. 1986.

[13] Traub, L. W., "Prediction of Vortex Breakdown and Longitudinal Characteristics of Swept Slender Planforms," *Journal of Aircraft*, Vol. 34, No. 3, 1997, pp. 353–359.

[14] *XFOIL Subsonic Airfoil Development System* [online database], http://web.mit.edu/drela/Public/web/xfoil/ [retrieved 10 Oct. 2007].